

# Photochemistry of $(\eta^5\text{-C}_5\text{H}_5)(\eta^5\text{-C}_4\text{H}_4\text{N})\text{Fe}$ and $(\eta^5\text{-C}_5\text{H}_5)(\eta^1\text{-N-C}_4\text{H}_4\text{N})\text{Fe}(\text{CO})_2$ in Low-Temperature Matrixes and Room-Temperature Solution. Evidence for a Photoinduced Haptotropic Shift of the $\pi$ -Coordinated Pyrrolyl Ligand

Davnat P. Heenan,<sup>†</sup> Conor Long,<sup>†</sup> Virginia Montiel-Palma,<sup>‡</sup>  
Robin N. Perutz,<sup>‡</sup> and Mary T. Pryce\*,<sup>†</sup>

*Inorganic Photochemistry Centre, Dublin City University, Dublin 9, Ireland, and Department of Chemistry, University of York, Heslington, York YO10 5DD, U.K.*

Received March 27, 2000

Azaferrocene,  $(\eta^5\text{-C}_5\text{H}_5)(\eta^5\text{-C}_4\text{H}_4\text{N})\text{Fe}$ , undergoes a  $\eta^5 \rightarrow \eta^1$  haptotropic shift of the pyrrolyl ligand upon long-wavelength photolysis ( $\lambda_{\text{exc}} > 495$  nm) both in alkane solvents at room temperature and in frozen matrixes at 12 K. Room-temperature photolysis ( $\lambda_{\text{exc}} > 495$  nm) in CO-saturated cyclohexane solution generated  $(\eta^5\text{-C}_5\text{H}_5)(\eta^1\text{-N-C}_4\text{H}_4\text{N})\text{Fe}(\text{CO})_2$ . Irradiation with  $\lambda_{\text{exc}} = 532$  nm also produced an allyl monocarbonyl species, *exo*- $(\eta^5\text{-C}_5\text{H}_5)(\eta^3\text{-C-C}_4\text{H}_4\text{N})\text{Fe}(\text{CO})$ , identified by IR spectroscopy. In CO-doped matrixes at 12 K both  $(\eta^5\text{-C}_5\text{H}_5)(\eta^1\text{-N-C}_4\text{H}_4\text{N})\text{Fe}(\text{CO})$  and  $(\eta^5\text{-C}_5\text{H}_5)(\eta^1\text{-N-C}_4\text{H}_4\text{N})\text{Fe}(\text{CO})_2$  are formed following broad-band irradiation ( $\lambda_{\text{exc}} > 495$  nm) of  $(\eta^5\text{-C}_5\text{H}_5)(\eta^5\text{-C}_4\text{H}_4\text{N})\text{Fe}$ , in a ratio dependent on the concentration of CO in the matrix. Initial irradiation with  $\lambda_{\text{exc}} = 538$  nm followed by broad-band photolysis ( $\lambda_{\text{exc}} > 495$  nm) in CO-doped matrixes formed additional monocarbonyl species, *exo*- $(\eta^5\text{-C}_5\text{H}_5)(\eta^3\text{-C-C}_4\text{H}_4\text{N})\text{Fe}(\text{CO})$ , and a species absorbing at  $1962\text{ cm}^{-1}$ , which is either the appropriate *endo*-isomer or aza-allyl species. Laser flash photolysis experiments of  $(\eta^5\text{-C}_5\text{H}_5)(\eta^1\text{-N-C}_4\text{H}_4\text{N})\text{Fe}(\text{CO})_2$  in either CO-saturated cyclohexane or toluene produced  $(\eta^5\text{-C}_5\text{H}_5)(\eta^1\text{-N-C}_4\text{H}_4\text{N})\text{Fe}(\text{CO})$ , which reacted with CO with rate constants measured at 298 K of  $(3.0 \pm 0.3) \times 10^8$  and  $(3.3 \pm 0.3) \times 10^8\text{ M}^{-1}\text{ s}^{-1}$ , respectively, regenerating  $(\eta^5\text{-C}_5\text{H}_5)(\eta^1\text{-N-C}_4\text{H}_4\text{N})\text{Fe}(\text{CO})_2$ .

## Introduction

The photochemical reactivity of half-sandwich compounds of the type  $(\eta^x\text{-aromatic ligand})\text{M}(\text{CO})_y$  ( $x = 4, 5$ , or  $6$ ;  $y = 2, 3$ , or  $4$ ;  $\text{M} = \text{V}, \text{Cr}, \text{Mn}$ , or  $\text{Co}$ ) can differ from the thermal chemistry.<sup>1,2</sup> For example,  $(\eta^6\text{-C}_6\text{H}_6)\text{-Cr}(\text{CO})_3$  undergoes thermally induced arene exchange, while CO loss is the dominant photochemical process.<sup>3,4</sup> Arene exchange proceeds via a thermally induced haptotropic shift of the  $\pi$ -ligand,<sup>3</sup> but to date the only report of a photoinduced haptotropic shift for these systems comes from our investigations into the photochemistry of  $\pi$ -coordinated pyridine compounds.<sup>5</sup> This work demonstrated that these processes occur following low-energy photolysis. For instance, photolysis of  $(\eta^6\text{-C}_5\text{H}_5\text{N})\text{Cr}(\text{CO})_3$  ( $\lambda_{\text{exc}} = 460$  nm) in a CO-doped methane matrix

at 10 K produced  $(\eta^1\text{-C}_5\text{H}_5\text{N})\text{Cr}(\text{CO})_5$ , while irradiation at 308 nm also produced the more familiar CO-loss product  $(\eta^6\text{-C}_5\text{H}_5\text{N})\text{Cr}(\text{CO})_2$ .

We have extended these studies to sandwich compounds related to ferrocene. Ferrocene is photoinert in dry alkane solvents, but it readily photooxidizes in haloalkanes.<sup>6</sup> Quantum yields for photodecomposition of ferrocene of up to unity are obtained in  $\text{CCl}_4/\text{EtOH}$  mixtures.<sup>6</sup> Substituted ferrocenes have been reported to photodecompose in solvents such as acetonitrile, methanol, DMSO, decalin, chloroform, or carbontetrachloride; the nature of this decomposition remains uncertain, however.<sup>7</sup> In all cases products are complex, and more recent work has suggested that the presence of traces of water is a prerequisite for photoactivity in some solvents.<sup>8</sup>

In this paper, we describe the photochemistry of azaferrocene,  $(\eta^5\text{-C}_5\text{H}_5)(\eta^5\text{-C}_4\text{H}_4\text{N})\text{Fe}$ , the closest and most accessible heterocyclic analogue of ferrocene. The reason for this study is primarily to determine if the photoinduced hapticity changes observed for  $\pi$ -coordinated pyridine, are also observed for  $\pi$ -coordinated

<sup>†</sup> Dublin City University.

<sup>‡</sup> University of York.

(1) Basolo, F. *New J. Chem.* **1994**, *18*, 19.

(2) O'Connor, J. M.; Casey, C. D. *Chem. Rev.* **1987**, *87*, 307.

(3) (a) Trayler, T. G.; Stewart, K. J.; Goldberg, M. J. *J. Am. Chem. Soc.* **1984**, *106*, 4445. (b) Trayler, T. G.; Stewart, K. J.; Goldberg, M. J. *Organometallics* **1986**, *5*, 2062. (c) Trayler, T. G.; Stewart, K. J. *J. Am. Chem. Soc.* **1986**, *108*, 6977. (d) Trayler, T. G.; Goldberg, M. J. *Organometallics* **1987**, *6*, 2413. (e) Trayler, T. G.; Goldberg, M. J. *Organometallics* **1987**, *6*, 2531.

(4) (a) Strohmeier, S.; von Hobe, D. Z. *Naturforsch.* **1963**, *18B*, 770. (b) Wrighton, M. S.; Haverty, J. L. Z. *Naturforsch.* **1975**, *30B*, 254. (c) Nasielski, J.; Denishoff, O. J. *Organomet. Chem.* **1975**, *102*, 65. (d) Gilbert, A.; Kelly, J. M.; Budzwait, M.; Koerner von Gustorf, E. Z. *Naturforsch.* **1976**, *31B*, 1091. (e) Rest, A. J.; Sodeau, J. R.; Taylor, D. J. *J. Chem. Soc., Dalton Trans.* **1978**, 651.

(5) Breheny, C. J.; Draper, S. M.; Grevels, F.-W.; Klotzbücher, W. E.; Long, C.; Pryce, M. T.; Russell, G. *Organometallics* **1996**, *15*, 3679.

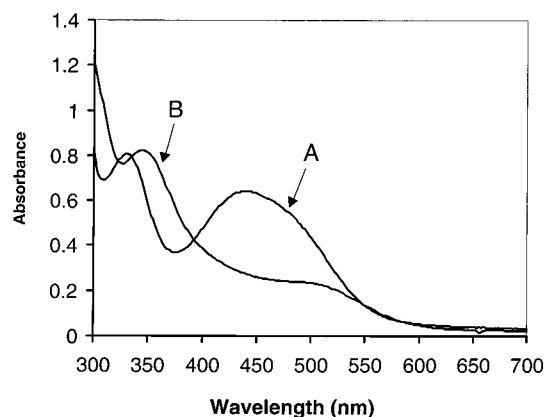
(6) Traverso, O.; Scandola, F. *Inorg. Chim. Acta* **1970**, *4*, 493. (b) Tarr, A. M.; Wiles, D. M. *Can. J. Chem.* **1968**, *46*, 2725. (c) von Gustorf, E. K.; Koller, H.; Jun, M.-J.; Schenck, G. O. *Chem.-Ing.-Tech.* **1963**, *35*, 591.

(7) (a) Ali, L. H.; Cox, A.; Kemp, T. S. *J. Chem. Soc., Dalton Trans.* **1973**, 1468. (b) Traverso, O.; Rossi, R.; Sostero, S.; Carassiti, V. *Mol. Photochem.* **1973**, *5*, 457.

(8) Davis, J.; Vaughan, D. H.; Cardosi, M. F. *Electroanalysis* **1997**, *9*, 650.

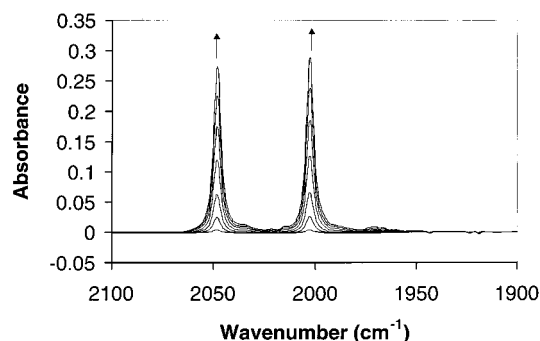
**Table 1.** Infrared Bands Observed in the CO Stretching Region for  $(\eta^5\text{-C}_5\text{H}_5)\text{Fe}(\text{CO})_2\text{X}$  Compounds and Their Photoproducts in Various Low-Temperature Matrixes and Room-Temperature Solution

complex	$\nu_{\text{CO}}$ ( $\text{cm}^{-1}$ )	medium
$(\eta^5\text{-C}_5\text{H}_5)(\eta^1\text{-C}_4\text{H}_4\text{N})\text{Fe}(\text{CO})_2$	2053, 2007	Ar matrix
$(\eta^5\text{-C}_5\text{H}_5)(\eta^1\text{-C}_4\text{H}_4\text{N})\text{Fe}(\text{CO})_2$	2052, 2006	$\text{N}_2$ matrix
$(\eta^5\text{-C}_5\text{H}_5)(\eta^1\text{-C}_4\text{H}_4\text{N})\text{Fe}(\text{CO})_2$	2048, 2002	$\text{C}_6\text{H}_{12}$
$(\eta^5\text{-C}_5\text{H}_5)(\eta^1\text{-C}_4\text{H}_4\text{N})\text{Fe}(\text{CO})$	1974	Ar matrix
$(\eta^5\text{-C}_5\text{H}_5)(\eta^1\text{-C}_4\text{H}_4\text{N})\text{Fe}(\text{CO})$	1974	$\text{N}_2$ matrix
$(\eta^5\text{-C}_5\text{H}_5)\text{Fe}(\text{CO})_2\text{Cl}^a$	2054, 2010	$\text{CH}_4$ matrix
$(\eta^5\text{-C}_5\text{H}_5)\text{Fe}(\text{CO})_2\text{Cl}^a$	2056, 2013	$\text{N}_2$ matrix
$(\eta^5\text{-C}_5\text{H}_5)\text{Fe}(\text{CO})\text{Cl}^a$	1977	$\text{CH}_4$ matrix
$(\eta^5\text{-C}_5\text{H}_5)\text{Fe}(\text{CO})\text{Cl}^a$	1979	$\text{N}_2$ matrix
$(\eta^5\text{-C}_5\text{H}_5)\text{Fe}(\text{CO})_2\text{I}^b$	2038, 2005	$\text{C}_6\text{H}_{12}$
$(\eta^5\text{-C}_5\text{H}_5)(\eta^3\text{-C}_3\text{H}_5)\text{Fe}(\text{CO})^c$	1950	$\text{CCl}_4$
$(\eta^5\text{-C}_5\text{H}_5)(\eta^3\text{-C}_4\text{H}_7)\text{Fe}(\text{CO})^c$	1949	thin film
$(\eta^5\text{-C}_5\text{H}_5)(\eta^3\text{-C-C}_4\text{H}_4\text{N})\text{Fe}(\text{CO})$	ca. 1949	$\text{C}_6\text{H}_{12}$
$(\eta^5\text{-C}_5\text{H}_5)(\eta^3\text{-C-C}_4\text{H}_4\text{N})\text{Fe}(\text{CO})$	1948	CO/Ar matrix
$(\eta^5\text{-C}_5\text{H}_5)(\eta^3\text{-N-C}_4\text{H}_4\text{N})\text{Fe}(\text{CO})$	1962	CO/Ar matrix

<sup>a</sup> Reference 17. <sup>b</sup> Reference 10. <sup>c</sup> Reference 11.**Figure 1.** UV/vis spectra for  $(\eta^5\text{-C}_5\text{H}_5)\text{Fe}(\eta^5\text{-C}_5\text{H}_5)$  ( $1.79 \times 10^{-2}$  M; spectrum A) and  $(\eta^5\text{-C}_5\text{H}_5)(\eta^1\text{-N-C}_4\text{H}_4\text{N})\text{Fe}(\text{CO})_2$  ( $5.91 \times 10^{-3}$  M; spectrum B) in cyclohexane.

pyrroles. The presence of the nitrogen atom in the  $\pi$ -coordinated ligand has a number of effects. The proximate nitrogen can act as an intramolecular "trap" for ring-slip intermediates. More fundamentally, its presence reduces the symmetry of the molecule. As a consequence, the degeneracy of valence orbitals, a feature of the homocyclic analogues, is lifted. This reduces the energy of low-energy excited states, permitting access to novel photochemical processes, such as haptotropic shift reactions.

The experimental results reported here were obtained using a combination of room-temperature techniques in dry cyclohexane solution and low-temperature matrix isolation methods. Evidence is presented to demonstrate that, in common with  $\eta^6$ -coordinated pyridine, the  $\eta^5$ -pyrrolyl ligand also undergoes facile photoinduced haptotropic shifts, opening multiple coordination sites on the metal center. Moreover, experiments using monochromatic irradiation indicate that the haptotropic shifts may occur by a stepwise  $\eta^5 \rightarrow \eta^3 \rightarrow \eta^1$  transformation involving the absorption of two photons. To assist with the assignment of intermediate species observed in these experiments, the photochemistry of  $(\eta^5\text{-C}_5\text{H}_5)(\eta^1\text{-N-C}_4\text{H}_4\text{N})\text{Fe}(\text{CO})_2$  was investigated by flash photolysis techniques in solution and also by matrix isolation.

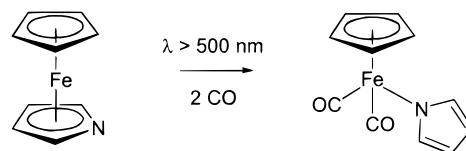
**Figure 2.** Spectral changes observed in the carbonyl region following photolysis ( $\lambda_{\text{exc}} > 500$  nm) of  $(\eta^5\text{-C}_5\text{H}_5)(\eta^5\text{-C}_4\text{H}_4\text{N})\text{Fe}$  in CO-saturated cyclohexane at room temperature, showing formation of  $(\eta^5\text{-C}_5\text{H}_5)(\eta^1\text{-N-C}_4\text{H}_4\text{N})\text{Fe}(\text{CO})_2$ .

## Results

The IR spectroscopic data for  $(\eta^5\text{-C}_5\text{H}_5)(\eta^5\text{-C}_4\text{H}_4\text{N})\text{Fe}$  and  $(\eta^5\text{-C}_5\text{H}_5)(\eta^1\text{-N-C}_4\text{H}_4\text{N})\text{Fe}(\text{CO})_2$  and their photoproducts are given in Table 1, while the UV/vis spectra of the starting materials in cyclohexane are represented in Figure 1. Both compounds exhibit weak absorptions in the visible region. The spectrum of  $(\eta^5\text{-C}_5\text{H}_5)(\eta^5\text{-C}_4\text{H}_4\text{N})\text{Fe}$  in cyclohexane contains features centered at 326 nm ( $\epsilon = 46 \text{ M}^{-1} \text{ cm}^{-1}$ ) and 423 nm ( $\epsilon = 38 \text{ M}^{-1} \text{ cm}^{-1}$ ), while  $(\eta^5\text{-C}_5\text{H}_5)(\eta^1\text{-N-C}_4\text{H}_4\text{N})\text{Fe}(\text{CO})_2$  has an absorption at 340 nm ( $\epsilon = 142 \text{ M}^{-1} \text{ cm}^{-1}$ ) and a weaker feature at 484 nm ( $\epsilon = 35 \text{ M}^{-1} \text{ cm}^{-1}$ ).

## Steady-State Photolysis Experiments

**Broad-Band Photolysis of  $(\eta^5\text{-C}_5\text{H}_5)(\eta^5\text{-C}_4\text{H}_4\text{N})\text{Fe}$  in CO-Saturated Cyclohexane Solution at Room Temperature.** Visible photolysis of a CO-saturated solution of  $(\eta^5\text{-C}_5\text{H}_5)(\eta^5\text{-C}_4\text{H}_4\text{N})\text{Fe}$  in cyclohexane with broad-band radiation from a xenon-arc lamp (275 W) fitted with a filter that only transmits wavelengths greater than 500 nm produced  $(\eta^5\text{-C}_5\text{H}_5)(\eta^1\text{-N-C}_4\text{H}_4\text{N})\text{Fe}(\text{CO})_2$  ( $\nu_{\text{CO}} = 2048$  and  $2002 \text{ cm}^{-1}$ , Table 1; reaction 1; Figure 2).<sup>9</sup> Experiments using a  $\lambda_{\text{exc}} > 400$  nm filter



also produced the dicarbonyl species as the major product, but small amounts of  $[(\eta^5\text{-C}_5\text{H}_5)\text{Fe}(\text{CO})_2]_2$  were formed in addition ( $\nu_{\text{CO}} = 1960$  and  $1793 \text{ cm}^{-1}$ ; the high-energy band at  $2002 \text{ cm}^{-1}$  is obscured by the low-energy absorption of  $(\eta^5\text{-C}_5\text{H}_5)(\eta^1\text{-N-C}_4\text{H}_4\text{N})\text{Fe}(\text{CO})_2$ ). In all cases the yield of the dinuclear species appeared low (based on IR band intensities), although it was greatest in experiments where the solution was simply flushed with CO rather than rigorously degassed by freeze-pump-thaw procedures followed by admission of CO to the solution cell. It should be noted that formation of

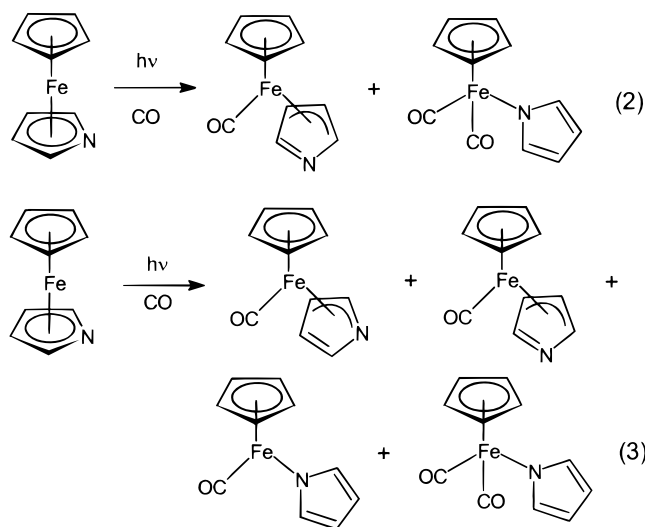
(9) (a) We have confirmed that this reaction is photochemical by control experiments in which the solution of  $(\eta^5\text{-C}_5\text{H}_5)(\eta^5\text{-C}_4\text{H}_4\text{N})\text{Fe}$  in CO-saturated cyclohexane was kept in the dark; no  $(\eta^5\text{-C}_5\text{H}_5)(\eta^1\text{-N-C}_4\text{H}_4\text{N})\text{Fe}(\text{CO})_2$  was formed under these conditions. (b) Martin, K. F.; Hanks, T. W. *Organometallics* **1997**, *16*, 4857.

the dinuclear species is also observed following photolysis of  $(\eta^5\text{-C}_5\text{H}_5)\text{Fe}(\text{CO})_2\text{I}$  in alkane solvents.<sup>10</sup>

**Broad-Band Photolysis of  $(\eta^5\text{-C}_5\text{H}_5)(\eta^5\text{-C}_4\text{H}_4\text{N})\text{Fe}$  in Degassed Cyclohexane Solution at Room Temperature.** Broad-band irradiation ( $\lambda_{\text{exc}} > 500$  nm) of a concentrated solution of  $(\eta^5\text{-C}_5\text{H}_5)(\eta^5\text{-C}_4\text{H}_4\text{N})\text{Fe}$  in degassed cyclohexane caused the solution to become turbid and eventually produced a precipitate. After the admission of CO, the precipitate slowly disappeared and the solution clarified. Monitoring of the solution by infrared spectroscopy indicated the formation (over several hours at room temperature) of bands at 2048 and 2002  $\text{cm}^{-1}$ , assigned to  $(\eta^5\text{-C}_5\text{H}_5)(\eta^1\text{-N-C}_4\text{H}_4\text{N})\text{Fe}(\text{CO})_2$ .

The observation of solution turbidity following irradiation in cyclohexane renders time-resolved studies on this system both difficult and prone to artifacts resulting from photoacoustic effects. As a consequence, the photochemistry of azaferrocene was not investigated by time-resolved techniques.

**Monochromatic Pulsed Photolysis of  $(\eta^5\text{-C}_5\text{H}_5)(\eta^5\text{-C}_4\text{H}_4\text{N})\text{Fe}$  in CO-Saturated Cyclohexane Solution at Room Temperature.** Pulsed photolysis of  $(\eta^5\text{-C}_5\text{H}_5)(\eta^5\text{-C}_4\text{H}_4\text{N})\text{Fe}$  in CO-saturated cyclohexane with  $\lambda_{\text{exc}} = 355$  nm produced  $(\eta^5\text{-C}_5\text{H}_5)(\eta^1\text{-N-C}_4\text{H}_4\text{N})\text{Fe}(\text{CO})_2$  as the sole carbonyl-containing product. However, pulsed photolysis using  $\lambda_{\text{exc}} = 532$  nm generated an additional species, with a single  $\nu_{\text{CO}}$  band at 1949  $\text{cm}^{-1}$  (Figure 3). We have assigned this band to  $(\eta^5\text{-C}_5\text{H}_5)(\eta^3\text{-C-C}_4\text{H}_4\text{N})\text{Fe}(\text{CO})$  (reaction 2), as it is close to that observed for  $(\eta^5\text{-C}_5\text{H}_5)(\eta^3\text{-C}_3\text{H}_5)\text{Fe}(\text{CO})$  or  $(\eta^5\text{-C}_5\text{H}_5)(\eta^3\text{-C}_4\text{H}_7)\text{Fe}(\text{CO})$  ( $\nu_{\text{CO}} = 1950$  or  $1948$   $\text{cm}^{-1}$  respectively) in  $\text{CCl}_4$  or as a thin film.<sup>11</sup>



### Matrix Isolation Studies

**Photolysis ( $\lambda_{\text{exc}} > 495$  nm) of  $(\eta^5\text{-C}_5\text{H}_5)(\eta^5\text{-C}_4\text{H}_4\text{N})\text{Fe}$  in Argon Matrixes at 12 K Containing Either 0.5% or 2% CO.** Azaferrocene exhibits UV/vis bands at 325 and 424 nm in a CO-doped argon matrix. Photolysis of  $(\eta^5\text{-C}_5\text{H}_5)(\eta^5\text{-C}_4\text{H}_4\text{N})\text{Fe}$  in these matrixes with  $\lambda_{\text{exc}} > 495$  nm produced two species, one with two  $\nu_{\text{CO}}$  bands of approximately equal intensity (2053 and 2008  $\text{cm}^{-1}$ )

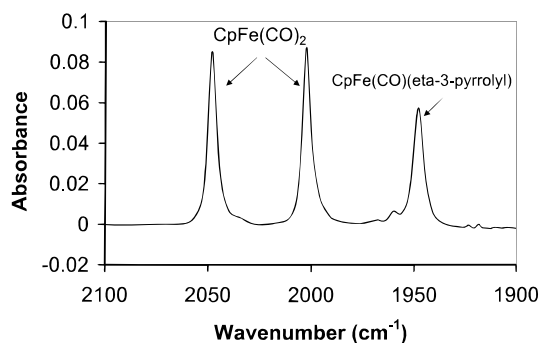


**Figure 3.** Infrared spectrum recorded after monochromatic irradiation ( $\lambda_{\text{exc}} = 532$  nm) of  $(\eta^5\text{-C}_5\text{H}_5)(\eta^5\text{-C}_4\text{H}_4\text{N})\text{Fe}$  in CO-saturated cyclohexane at room temperature.  $\text{CpFe}(\text{CO})_2 = (\eta^5\text{-C}_5\text{H}_5)(\eta^1\text{-N-C}_4\text{H}_4\text{N})\text{Fe}(\text{CO})_2$ ;  $\text{CpFe}(\text{CO})(\eta^3\text{-pyrrolyl}) = (\eta^5\text{-C}_5\text{H}_5)(\eta^3\text{-C-C}_4\text{H}_4\text{N})\text{Fe}(\text{CO})$ .

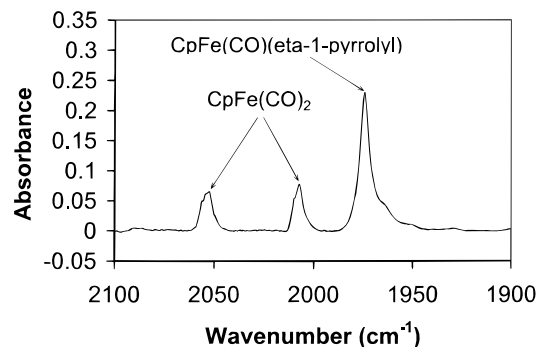


**Figure 4.** Infrared spectrum recorded following photolysis ( $\lambda_{\text{exc}} > 500$  nm) of  $(\eta^5\text{-C}_5\text{H}_5)(\eta^5\text{-C}_4\text{H}_4\text{N})\text{Fe}$  in 0.5% CO/Ar matrix at 12 K.  $\text{CpFe}(\text{CO})_2 = (\eta^5\text{-C}_5\text{H}_5)(\eta^1\text{-N-C}_4\text{H}_4\text{N})\text{Fe}(\text{CO})_2$ ;  $\text{CpFe}(\text{CO})(\eta^1\text{-pyrrolyl}) = (\eta^5\text{-C}_5\text{H}_5)(\eta^1\text{-N-C}_4\text{H}_4\text{N})\text{Fe}(\text{CO})$ .

and the other with a single band at 1974  $\text{cm}^{-1}$  (Figure 4).<sup>12</sup> The ratio of the intensity of these product bands varied with the concentration of CO in the matrix. For instance, the band at 1974  $\text{cm}^{-1}$  band was 4 times as intense as that at 2053 and 2008  $\text{cm}^{-1}$  for a matrix containing 0.5% CO, while it was only twice as large in a 2% CO matrix. Within individual experiments, this ratio remained constant.

The species absorbing at 2053 and 2008  $\text{cm}^{-1}$  was assigned to  $(\eta^5\text{-C}_5\text{H}_5)(\eta^1\text{-N-C}_4\text{H}_4\text{N})\text{Fe}(\text{CO})_2$  by comparison with the infrared spectrum of an authentic sample of  $(\eta^5\text{-C}_5\text{H}_5)(\eta^1\text{-N-C}_4\text{H}_4\text{N})\text{Fe}(\text{CO})_2$  in the same matrix (cf. Table 1).<sup>13</sup> The band at 1974  $\text{cm}^{-1}$  was assigned to the 16-electron  $(\eta^5\text{-C}_5\text{H}_5)(\eta^1\text{-N-C}_4\text{H}_4\text{N})\text{Fe}(\text{CO})$  species (a strong absorption at 415 nm, a shoulder at 317 nm, and a weak broad feature at ca. 730–750 nm correlate with this IR band), and support for this assignment came from matrix experiments on  $(\eta^5\text{-C}_5\text{H}_5)(\eta^1\text{-N-C}_4\text{H}_4\text{N})\text{Fe}(\text{CO})_2$ , which produced  $(\eta^5\text{-C}_5\text{H}_5)(\eta^1\text{-N-C}_4\text{H}_4\text{N})\text{Fe}(\text{CO})$  and free CO on photolysis (see below). The band at 1975  $\text{cm}^{-1}$  is asymmetric, with two further unresolved components at 1962 and 1948  $\text{cm}^{-1}$  (see below for assignments).

(12) The 1975  $\text{cm}^{-1}$  band also exhibited shoulders to the low-energy side at ca. 1962 and 1948  $\text{cm}^{-1}$ , possibly indicating the formation of further carbonyl-containing species.

(13) It should be noted that the values for the  $\nu_{\text{CO}}$  bands for  $(\eta^5\text{-C}_5\text{H}_5)(\eta^1\text{-N-C}_4\text{H}_4\text{N})\text{Fe}(\text{CO})_2$  quoted in the literature are incorrect. We have confirmed our values by correlating our infrared spectral data obtained from a single sample of the compound with the results of high-resolution mass spectrometry and single-crystal X-ray diffraction techniques.

(10) Pan, X.; Philbin, C. E.; Castellani, M. P.; Tyler, D. R. *Inorg. Chem.* **1988**, *27*, 671.

(11) Green, M. L. H.; Nagy, P. L. I. *J. Chem. Soc.* **1963**, 189.



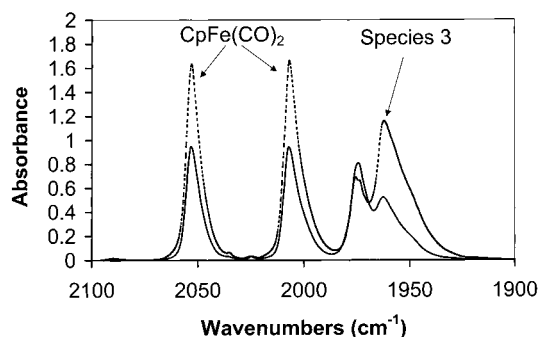
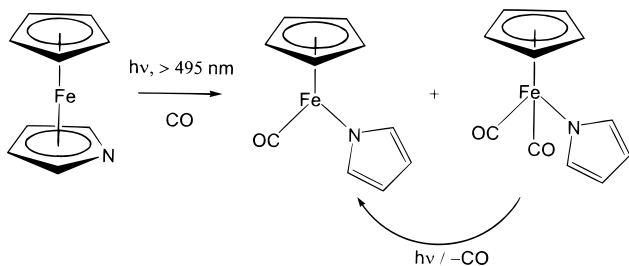


**Figure 5.** Infrared spectra following photolysis of  $(\eta^5\text{-C}_5\text{H}_5)(\eta^5\text{-C}_4\text{H}_4\text{N})\text{Fe}$  in a 2% CO/Ar matrix at 12 K (a) at  $\lambda_{\text{exc}} = 538$  nm for 200 min (—) and (b) subsequent photolysis at  $\lambda_{\text{exc}} > 495$  nm (---).

**Scheme 1. Broad-Band Matrix Photolysis of  $(\eta^5\text{-C}_5\text{H}_5)(\eta^5\text{-N-C}_4\text{H}_4\text{N})\text{Fe}$  and  $(\eta^5\text{-C}_5\text{H}_5)(\eta^1\text{-N-C}_4\text{H}_4\text{N})\text{Fe}(\text{CO})_2$**



**Initial Photolysis ( $\lambda_{\text{exc}} > 495$  nm) of  $(\eta^5\text{-C}_5\text{H}_5)(\eta^5\text{-C}_4\text{H}_4\text{N})\text{Fe}$  in Argon Matrixes at 12 K, Containing Either 0.5% CO or 2% CO, and Subsequent Broad-Band Photolysis ( $\lambda_{\text{exc}} > 325$  nm).** Initial photolysis of an argon matrix containing  $(\eta^5\text{-C}_5\text{H}_5)(\eta^5\text{-C}_4\text{H}_4\text{N})\text{Fe}$  again produced the two carbonyl-containing species as outlined above. Changing to shorter wavelengths resulted in a change in ratio of the product bands, the intensity of the band at  $1974\text{ cm}^{-1}$  increasing more rapidly than those at  $2053$  and  $2008\text{ cm}^{-1}$ . This suggests that the dicarbonyl product is undergoing photoinduced CO loss at these excitation wavelengths (Scheme 1). This was confirmed by matrix and time-resolved experiments on  $(\eta^5\text{-C}_5\text{H}_5)(\eta^1\text{-N-C}_4\text{H}_4\text{N})\text{Fe}(\text{CO})_2$  (see below).

**Monochromatic Photolysis ( $\lambda_{\text{exc}} = 538$  nm) of  $(\eta^5\text{-C}_5\text{H}_5)(\eta^5\text{-C}_4\text{H}_4\text{N})\text{Fe}$  in Argon Matrixes at 12 K Containing 2% CO and Subsequent Broad-Band Photolysis with  $\lambda_{\text{exc}} > 495$  nm.** In contrast with the matrix experiments described above, where samples were irradiated with broad-band light sources, monochromatic irradiation of  $(\eta^5\text{-C}_5\text{H}_5)(\eta^5\text{-C}_4\text{H}_4\text{N})\text{Fe}$  in a CO-doped argon matrix with  $\lambda_{\text{exc}} = 538$  nm produced four carbonyl-containing species (Figure 5a). In addition to  $(\eta^5\text{-C}_5\text{H}_5)(\eta^1\text{-N-C}_4\text{H}_4\text{N})\text{Fe}(\text{CO})_2$  and  $(\eta^5\text{-C}_5\text{H}_5)(\eta^1\text{-N-C}_4\text{H}_4\text{N})\text{Fe}(\text{CO})$  previously observed, further species with  $\nu_{\text{CO}} = 1962$  and  $1948\text{ cm}^{-1}$  were formed, the identity of which will be discussed later. Subsequent irradiation of this matrix with  $\lambda_{\text{exc}} > 495$  nm resulted in a substantial increase in the intensity of the bands at  $2053$ ,  $2008$ ,  $1962$ , and  $1948\text{ cm}^{-1}$ , while the intensity of the band assigned to  $(\eta^5\text{-C}_5\text{H}_5)(\eta^1\text{-N-C}_4\text{H}_4\text{N})\text{Fe}(\text{CO})$  decreased slightly (Figure 5b). This experiment and related ones showed a feature at  $660\text{ nm}$  in the UV/vis spectrum (Figure 6) which is associated with the species absorbing at  $1962$  and  $1948\text{ cm}^{-1}$  in the infrared spectrum.

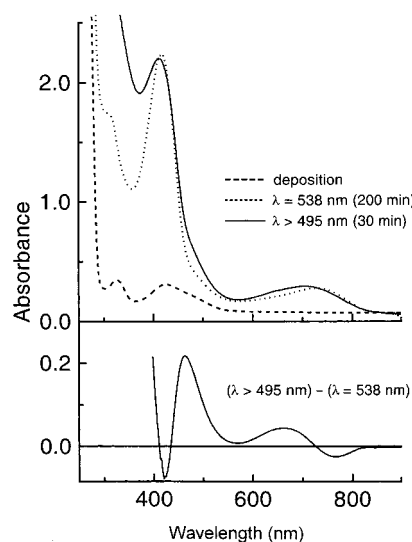


**Figure 6.** UV/vis spectra following photolysis of  $(\eta^5\text{-C}_5\text{H}_5)(\eta^5\text{-C}_4\text{H}_4\text{N})\text{Fe}$  in a 2% CO/Ar matrix at 12 K, (a) following deposition (---), (b) at  $\lambda_{\text{exc}} = 538$  nm (200 min; ···), and (c) subsequent photolysis at  $\lambda_{\text{exc}} > 495$  nm (30 min; —).

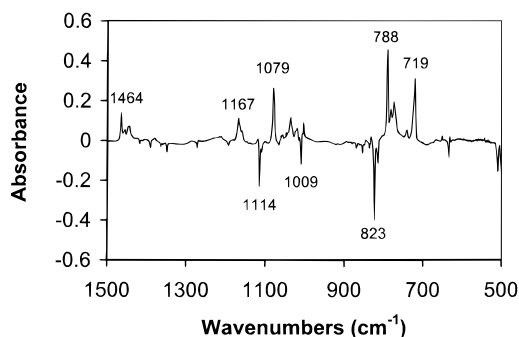


**Figure 7.** IR difference spectrum obtained following photolysis ( $\lambda_{\text{exc}} > 495$  nm) of  $(\eta^5\text{-C}_5\text{H}_5)(\eta^5\text{-C}_4\text{H}_4\text{N})\text{Fe}$  in an argon matrix at 12 K.

**Photolysis of  $(\eta^5\text{-C}_5\text{H}_5)(\eta^5\text{-C}_4\text{H}_4\text{N})\text{Fe}$  in an Argon or a Nitrogen Matrix at 12 K.** The spectroscopic changes observed following photolysis of  $(\eta^5\text{-C}_5\text{H}_5)(\eta^5\text{-C}_4\text{H}_4\text{N})\text{Fe}$  ( $\lambda_{\text{exc}} > 495$  nm) in an argon matrix are presented in Figure 7. We have assigned these changes to the depletion of  $(\eta^5\text{-C}_5\text{H}_5)(\eta^5\text{-C}_4\text{H}_4\text{N})\text{Fe}$  and the formation of a ring-slip product. The nature of the coordination mode of the pyrrolyl ligand is uncertain. However ab initio calculations on  $(\eta^5\text{-C}_5\text{H}_5)(\eta^1\text{-N-C}_4\text{H}_4\text{N})\text{Fe}$  were undertaken to estimate the infrared properties of this 14-electron species. The starting geometry was based on the molecular structure published for  $(\eta^5\text{-C}_5\text{H}_5)(\eta^1\text{-N-C}_4\text{H}_4\text{N})\text{Fe}(\text{CO})_2$ <sup>14</sup> but with both carbonyl ligands removed from the atom list. A full geometry optimization was undertaken at B3LYP/LANL2DZ model chemistry using the Gaussian-98 program suite.<sup>15</sup> The Hessian matrix, again calculated using the same model chemistry, revealed only one trivial negative frequency ( $-55\text{ cm}^{-1}$ ) associated with the rotation of the  $(\eta^5\text{-C}_5\text{H}_5)$  ligand. The results of these calculations together with the observed band positions are presented in Table 2.<sup>16</sup> On the basis of these results we can assign the spectral features observed in these matrix experiments to  $(\eta^5\text{-C}_5\text{H}_5)(\eta^1\text{-N-C}_4\text{H}_4\text{N})\text{Fe}$ . Photolyses in a dinitrogen matrix

(14) Powell, M. A.; Bailey, R. D.; Eagle, C. T.; Schimel, G. L.; Hanks, T. W.; Pennington, W. T. *Acta Crystallogr.* **1997**, C53, 1611.

**Table 2. Observed (for photolysis product of azaferrocene in argon matrixes) and Calculated Band Positions for  $(\eta^5\text{-C}_5\text{H}_5)(\eta^1\text{-N-C}_4\text{H}_4\text{N})\text{Fe}$  Based on an Optimized Geometry at B3LYP/LANL2DZ Model Chemistry<sup>a</sup>**

observed band positions (cm <sup>-1</sup> )	calculated band positions (cm <sup>-1</sup> )
719	715
772	749
781	763
788	777
831	834
1035	1009
	1012
	1023
1079	1049
	1055
1167	1142
	1154
1464	1440

<sup>a</sup> The calculated values have been corrected using an empirical factor of 0.98 (see ref 16).

gave rise to spectral changes, essentially identical to those observed in an argon matrix.

**Photolysis of  $(\eta^5\text{-C}_5\text{H}_5)(\eta^1\text{-N-C}_4\text{H}_4\text{N})\text{Fe}(\text{CO})_2$  in Argon and Dinitrogen Matrixes at 12 K.** Photolysis ( $\lambda_{\text{exc}} > 400$  nm) of  $(\eta^5\text{-C}_5\text{H}_5)(\eta^1\text{-N-C}_4\text{H}_4\text{N})\text{Fe}(\text{CO})_2$  in an argon matrix at 12 K resulted in the depletion of the parent bands (2053 and 2007 cm<sup>-1</sup>) and the formation of new bands at 2134 and 1974 cm<sup>-1</sup> (the 1974 cm<sup>-1</sup> band exhibited shoulders on the low-energy side).<sup>12</sup> These bands are assigned to free CO and  $(\eta^5\text{-C}_5\text{H}_5)(\eta^1\text{-N-C}_4\text{H}_4\text{N})\text{Fe}(\text{CO})$ , respectively. The spectral changes observed in a dinitrogen matrix were identical to those in an argon matrix. This suggests that  $(\eta^5\text{-C}_5\text{H}_5)(\eta^1\text{-N-C}_4\text{H}_4\text{N})\text{Fe}(\text{CO})$  does not react with dinitrogen. The matrix photochemistry of  $(\eta^5\text{-C}_5\text{H}_5)\text{Fe}(\text{CO})_2\text{Cl}$  reported by Rest and co-workers<sup>17</sup> also identified CO loss as the dominant photochemical process, and the resulting monocarbonyl  $(\eta^5\text{-C}_5\text{H}_5)\text{Fe}(\text{CO})\text{Cl}$  species was inert to dinitrogen (exhibiting similar band positions in both methane and nitrogen matrixes,  $\nu_{\text{CO}} = 1977$  and 1979 cm<sup>-1</sup>, respectively).

**UV/Vis Flash Photolysis Experiments of  $(\eta^5\text{-C}_5\text{H}_5)(\eta^1\text{-N-C}_4\text{H}_4\text{N})\text{Fe}(\text{CO})_2$  in Cyclohexane or Toluene Solution at Room Temperature.** Flash photolysis of  $(\eta^5\text{-C}_5\text{H}_5)(\eta^1\text{-N-C}_4\text{H}_4\text{N})\text{Fe}(\text{CO})_2$  produced a transient species with a  $\lambda_{\text{max}}$  at approximately 430 nm ( $\lambda_{\text{exc}} = 355$  nm) assigned to  $(\eta^5\text{-C}_5\text{H}_5)(\eta^1\text{-N-C}_4\text{H}_4\text{N})\text{Fe}(\text{CO})$ . A typical transient signal in CO-saturated cyclohexane

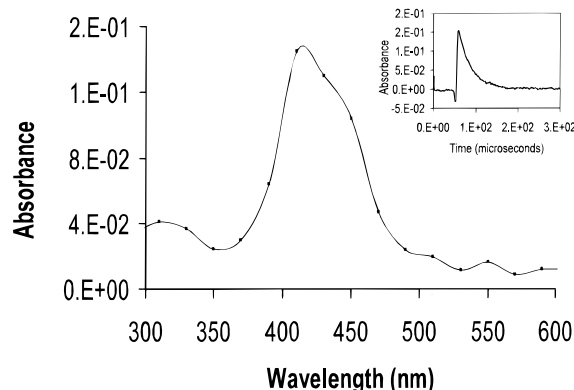
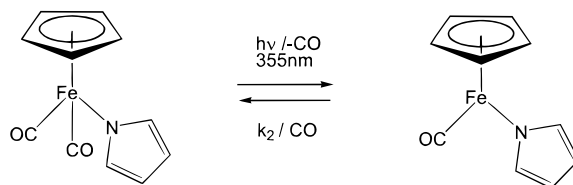


**Figure 8.** UV/vis difference transient absorption spectrum obtained after 2  $\mu\text{s}$  following photolysis of  $(\eta^5\text{-C}_5\text{H}_5)(\eta^1\text{-N-C}_4\text{H}_4\text{N})\text{Fe}(\text{CO})_2$  at  $\lambda_{\text{exc}} = 355$  nm in cyclohexane under 1 atm of CO. The inset shows a typical transient signal observed at 420 nm.

**Scheme 2. Flash Photolysis of  $(\eta^5\text{-C}_5\text{H}_5)(\eta^1\text{-N-C}_4\text{H}_4\text{N})\text{Fe}(\text{CO})_2$  Resulting in Decarbonylation Followed by Rapid Recombination with CO**



and a difference spectrum are given in Figure 8. Under these conditions, this species decays to the preirradiation baseline in less than 2  $\mu\text{s}$ , indicating that the process is reversible. The steady-state UV/vis spectrum of the photolysis solution was monitored throughout the experiment and showed no significant change, confirming that the overall process is reversible.

A plot of the observed rate constant ( $k_{\text{obs}}$ ) for the decay of the transient species against  $[\text{CO}]$  was linear. The slope of this plot gave the second-order rate constant ( $k_2$ ) of  $(3.0 \pm 0.3) \times 10^8 \text{ M}^{-1} \text{ s}^{-1}$  at 298 K for the reaction of  $(\eta^5\text{-C}_5\text{H}_5)(\eta^1\text{-N-C}_4\text{H}_4\text{N})\text{Fe}(\text{CO})$  with CO. Flash photolysis in CO-saturated toluene again produced a transient species with a maximum centered at 430 nm which reacted with CO with a similar rate constant of  $(3.3 \pm 0.3) \times 10^8 \text{ M}^{-1} \text{ s}^{-1}$  (see Scheme 2). These results indicate that neither the alkane nor the aromatic solvents interact to any significant extent with  $(\eta^5\text{-C}_5\text{H}_5)(\eta^1\text{-N-C}_4\text{H}_4\text{N})\text{Fe}(\text{CO})$ .

## Discussion

In contrast with ferrocene,  $(\eta^5\text{-C}_5\text{H}_5)(\eta^5\text{-C}_4\text{H}_4\text{N})\text{Fe}$  is photoactive in dry hydrocarbon solvents. Broad-band photolysis of  $(\eta^5\text{-C}_5\text{H}_5)(\eta^5\text{-C}_4\text{H}_4\text{N})\text{Fe}$  at  $\lambda_{\text{exc}} > 500$  nm in degassed cyclohexane at room temperature produced a precipitate together with turbidity and a deepening of the solution color. Subsequent addition of CO to the photolyzed solution yielded  $(\eta^5\text{-C}_5\text{H}_5)(\eta^1\text{-N-C}_4\text{H}_4\text{N})\text{Fe}(\text{CO})_2$  over several hours, presumably by the slow reaction of CO with the precipitate. Attempts to isolate and characterize this precipitate failed.

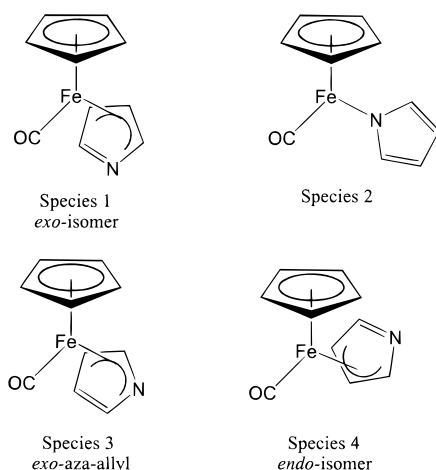
Broad-band photolysis ( $\lambda_{\text{exc}} > 500$  nm) of a CO-saturated cyclohexane solution ( $[\text{CO}] = 9.0 \times 10^{-3} \text{ M}$ )

(15) Frisch, M. J.; Trucks, G. W.; Schlegel, H. B.; Scuseria, G. E.; Robb, M. A.; Cheeseman, M. R.; Zakrzewski, V. G.; Montgomery, J. A., Jr.; Stratmann, R. E.; Burant, J. C.; Dapprich, S.; Millam, J. M.; Daniels, A. D.; Kudin, K. N.; Strain, M. C.; Farkas, O.; Tomasi, J.; Barone, V.; Cossi, M.; Cammi, R.; Mennucci, B.; Pomelli, C.; Adamo, C.; Clifford, S.; Ochterski, J.; Petersson, G. A.; Ayala, P. Y.; Cui, Q.; Morokuma, K.; Malick, D. K.; Abuck, A. D.; Raghavachari, K.; Foresman, J. B.; Cioslowski, J.; Ortiz, J. V.; Stefanov, B. B.; Liu, G.; Liashenko, A.; Piskorz, P.; Komaromi, I.; Gomperts, R.; Martin, R. L.; Fox, D. J.; Keith, T.; Al-Laham, M. A.; Peng, C. Y.; Nanayakkara, A.; Gonzalez, C.; Challacombe, M.; Gill, P. M. W.; Johnson, B.; Chen, W.; Wong, M. W.; Andres, J. L.; Gonzalez, C.; Head-Gordon, M.; Replogle, E. S.; Pople, J. A. *Gaussian 98*, Revision A.3; Gaussian, Inc.: Pittsburgh, PA, 1998.

(16) The calculated band positions were corrected using a factor of 0.98, derived from calculations using the same model chemistry on half-sandwich compounds of the type  $(\eta^6\text{-arene})\text{Cr}(\text{CO})_3$ , which exhibit unambiguous spectral features particularly in the  $\nu_{\text{CO}}$  region.

(17) Hooker, R. H.; Mahmoud, K. A.; Rest, A. J. *J. Chem. Soc., Dalton Trans.* **1990**, 1231.

of  $(\eta^5\text{-C}_5\text{H}_5)(\eta^5\text{-C}_4\text{H}_4\text{N})\text{Fe}$  formed  $(\eta^5\text{-C}_5\text{H}_5)(\eta^1\text{-N-C}_4\text{H}_4\text{N})\text{Fe}(\text{CO})_2$ , confirming that the  $\eta^5$ -coordinated pyrrolyl ligand undergoes a photoinduced haptotropic shift reaction. Another carbonyl compound, observed only following monochromatic irradiation at 532 nm, was identified as the *exo*-isomer of  $(\eta^5\text{-C}_5\text{H}_5)(\eta^3\text{-C-C}_4\text{H}_4\text{N})\text{Fe}(\text{CO})$  (species 1). This assignment was based on a comparison of



its  $\nu_{\text{CO}}$  band ( $1948\text{ cm}^{-1}$ ) with that of  $(\eta^5\text{-C}_5\text{H}_5)(\eta^3\text{-C}_3\text{H}_5)\text{Fe}(\text{CO})$  ( $1950\text{ cm}^{-1}$ ).<sup>11</sup> The observation of what appears to be an intermediate  $\eta^3$  species suggests that two photons are required for the overall  $\eta^5$ -to- $\eta^1$  transformation. Indeed, subsequent broad-band visible photolysis of the  $\eta^3$ -intermediate indicates that it is photosensitive, presumably yielding the  $\eta^1$  species. However it is not possible to be certain of this, as the additional dicarbonyl species produced could be the result of further photolysis of the parent species still present in solution.

Matrix experiments on  $(\eta^5\text{-C}_5\text{H}_5)(\eta^5\text{-C}_4\text{H}_4\text{N})\text{Fe}$  were performed to identify the nature of ring-slip intermediates. These experiments can be divided into two groups, those in which the isolating matrix is inert and those in which the matrix material reacts with the photofragments. For this system dinitrogen, frequently used as a reactive matrix, is inert. Consequently, active matrixes used consisted of various concentrations (expressed as %) of CO in argon. Coordination of CO to the photofragments provided information on their nature by examination of the  $\nu_{\text{CO}}$  absorption bands.

Long-wavelength ( $\lambda_{\text{exc}} > 495\text{ nm}$ ) photolysis of  $(\eta^5\text{-C}_5\text{H}_5)(\eta^5\text{-C}_4\text{H}_4\text{N})\text{Fe}$  in an argon matrix resulted in depletion of the infrared bands of the parent compound, and the formation of new bands in the fingerprint region (Figure 7). Because the photoproduct(s) lack diagnostic spectroscopic features, we calculated the IR spectrum of a likely product by DFT methods. The band positions calculated for  $(\eta^5\text{-C}_5\text{H}_5)(\eta^1\text{-C}_4\text{H}_4\text{N})\text{Fe}$  provide the best match to those observed in the matrix experiment (Table 2). As mentioned above, experiments in a dinitrogen matrix produced almost identical spectral changes to those observed in argon, with no evidence for species with coordinated dinitrogen.

Experiments using CO-doped matrixes provided considerably more information on the nature of the photoproducts. In these experiments, both  $(\eta^5\text{-C}_5\text{H}_5)(\eta^1\text{-N-C}_4\text{H}_4\text{N})\text{Fe}(\text{CO})_2$  and  $(\eta^5\text{-C}_5\text{H}_5)(\eta^1\text{-N-C}_4\text{H}_4\text{N})\text{Fe}(\text{CO})$  (species 2) were identified following low-energy broad-band photolysis of  $(\eta^5\text{-C}_5\text{H}_5)(\eta^5\text{-C}_4\text{H}_4\text{N})\text{Fe}$  in both 0.5%

and 2% CO in argon matrixes at 12 K. The former assignment was based on the known  $\nu_{\text{CO}}$  band positions for  $(\eta^5\text{-C}_5\text{H}_5)(\eta^1\text{-N-C}_4\text{H}_4\text{N})\text{Fe}(\text{CO})_2$  in the same matrix (Table 1). The latter depended on its similarity to the spectroscopic properties of  $(\eta^5\text{-C}_5\text{H}_5)\text{Fe}(\text{CO})\text{Cl}$  measured by Rest and co-workers (Table 1)<sup>17</sup> and the results of our investigations of the photochemistry of  $(\eta^5\text{-C}_5\text{H}_5)(\eta^1\text{-C}_4\text{H}_4\text{N})\text{Fe}(\text{CO})_2$  reported here. Experimental data in the literature confirm that a  $\eta^1$ -N-coordinated pyrrolyl ligand has electronic properties similar to those of the halogens, resulting in similar  $\nu_{\text{CO}}$  frequencies (Table 1).<sup>17,18</sup>

In low-temperature matrixes the monocarbonyl and dicarbonyl species were formed concomitantly and in the same ratio throughout the photolysis with  $\lambda > 495\text{ nm}$ . This observation suggests that they were both formed by the reaction of CO with a single photoproduct, i.e., the 14-electron species  $(\eta^5\text{-C}_5\text{H}_5)(\eta^1\text{-N-C}_4\text{H}_4\text{N})\text{Fe}$ . The observation that the ratio of mono- to dicarbonyl products was strongly dependent on the concentration of CO further supported this conclusion, the relative yield of the dicarbonyl species being greatest in matrixes containing a greater concentration of CO.

The  $\nu_{\text{CO}}$  band ( $1974\text{ cm}^{-1}$ ) of  $(\eta^5\text{-C}_5\text{H}_5)(\eta^1\text{-N-C}_4\text{H}_4\text{N})\text{Fe}(\text{CO})$  was asymmetric (Figure 4). This was true whether the monocarbonyl species was formed by photolysis of  $(\eta^5\text{-C}_5\text{H}_5)(\eta^5\text{-C}_4\text{H}_4\text{N})\text{Fe}$  in a CO-doped matrix or from  $(\eta^5\text{-C}_5\text{H}_5)(\eta^1\text{-N-C}_4\text{H}_4\text{N})\text{Fe}(\text{CO})_2$  in an argon matrix. The shoulders on the low-energy side indicated the presence of further CO-containing species rather than a matrix effect, as only this band exhibited the asymmetry. The species absorbing at approximately  $1948\text{ cm}^{-1}$  was assigned to  $(\eta^5\text{-C}_5\text{H}_5)(\eta^3\text{-C-C}_4\text{H}_4\text{N})\text{Fe}(\text{CO})$  (species 1) on the basis of the observation of a similar band in the room-temperature photolysis of  $(\eta^5\text{-C}_5\text{H}_5)(\eta^5\text{-C}_4\text{H}_4\text{N})\text{Fe}$  in CO-saturated cyclohexane (see above). The species absorbing at  $1962\text{ cm}^{-1}$  is more difficult to assign however. This species could be either the aza-allyl isomer  $(\eta^5\text{-C}_5\text{H}_5)(\eta^3\text{-N-C}_4\text{H}_4\text{N})\text{Fe}(\text{CO})$  or alternatively the *endo*-isomer of  $(\eta^5\text{-C}_5\text{H}_5)(\eta^3\text{-C-C}_4\text{H}_4\text{N})\text{Fe}(\text{CO})$  (species 3 and 4, respectively). It is generally accepted that the *endo*-isomers of allyl compounds are less stable than the *exo*-isomers and that the carbonyl stretching absorptions of the *endo*-isomers occur at lower energy than those of *exo*-isomers. Consequently, an assignment of the  $1962\text{ cm}^{-1}$  band to species 4 is not consistent with previously published data for related systems,<sup>19,20</sup> and we favor the assignment of the  $1962\text{ cm}^{-1}$  band to species 3.

The yield of the species absorbing at  $1962\text{ cm}^{-1}$  was significantly increased by initially using monochromatic irradiation ( $\lambda_{\text{exc}} = 538\text{ nm}$ ) followed by broad-band photolysis ( $\lambda_{\text{exc}} > 495\text{ nm}$ ) (Figure 5). This suggests that monochromatic irradiation of  $(\eta^5\text{-C}_5\text{H}_5)(\eta^5\text{-C}_4\text{H}_4\text{N})\text{Fe}$  produced a precursor species, containing an  $\eta^3$ -coordinated pyrrolyl ligand, which then reacted with CO, producing the observed species. Therefore, the ultimate observation of a particular carbonyl-containing species is dependent on the initial photolysis wavelength because all precursor species are themselves photoactive.

(18) Alway, D. G.; Barnett, K. W. *Inorg. Chem.* **1978**, *17*, 2826.

(19) Belmont, J. A.; Wrighton, M. S. *Organometallics* **1986**, *5*, 1421.

(20) Fish, R. W.; Giering, W. P.; Marten, D.; Rosenblum, M. J. *Organomet. Chem.* **1976**, *105*, 101.



Laser flash photolysis of  $(\eta^5\text{-C}_5\text{H}_5)(\eta^1\text{-N-C}_4\text{H}_4\text{N})\text{Fe}(\text{CO})_2$  produced a transient species with a  $\lambda_{\text{max}}$  centered at 420 nm. The primary photoproduct in solution was confirmed as the 16-electron CO-loss species. The observed rate constant for its reaction with CO varied linearly with [CO], providing estimates of the second-order rate constant of  $(3.0 \pm 0.3) \times 10^8 \text{ M}^{-1} \text{ s}^{-1}$  in cyclohexane and  $(3.3 \pm 0.3) \times 10^8 \text{ M}^{-1} \text{ s}^{-1}$  in toluene at 298 K. The magnitude of the second-order rate constants indicates that this intermediate does not interact with the solvent to any significant extent. This is in contrast with 16-electron species of the group 6 metals. For instance, the rate of displacement of solvent by CO in  $(\eta^6\text{-C}_6\text{H}_6)\text{Cr}(\text{CO})_2(\text{toluene})$ <sup>21</sup> is an order of magnitude slower than that for  $(\eta^6\text{-C}_6\text{H}_6)\text{Cr}(\text{CO})_2(\text{cyclohexane})$ .<sup>22</sup>

These experiments confirmed that  $(\eta^5\text{-C}_5\text{H}_5)(\eta^1\text{-N-C}_4\text{H}_4\text{N})\text{Fe}(\text{CO})_2$  undergoes photoinduced CO loss following photolysis at 355 nm, which in turn explains why the ratios of  $(\eta^5\text{-C}_5\text{H}_5)(\eta^1\text{-N-C}_4\text{H}_4\text{N})\text{Fe}(\text{CO})$  to  $(\eta^5\text{-C}_5\text{H}_5)(\eta^1\text{-N-C}_4\text{H}_4\text{N})\text{Fe}(\text{CO})_2$  formed following photolysis of  $(\eta^5\text{-C}_5\text{H}_5)(\eta^5\text{-C}_4\text{H}_4\text{N})\text{Fe}$  in CO-doped argon matrixes varied with photolysis time when  $\lambda_{\text{exc}} > 325 \text{ nm}$  was used. With photons of these wavelengths the dicarbonyl product undergoes a photoinduced decarbonylation.

### Concluding Remarks

This study demonstrates that  $(\eta^5\text{-C}_5\text{H}_5)(\eta^5\text{-N-C}_4\text{H}_4\text{N})\text{Fe}$  has an extensive photochemistry which is dominated by haptotropic shifts of the coordinated pyrrolyl ligand. A photoinduced stepwise shift from  $\eta^5$  through  $\eta^3$  ultimately yields an  $\eta^1$ -coordinated species. The relative importance of the various intermediates is strongly dependent on the photolysis conditions. This reflects the photosensitive nature of many of the intermediates formed. The coordinatively unsaturated intermediates also appear to be discriminating with what they will react, a feature also observed with other iron systems. The ability of the pyrrolyl ligand to adopt a variety of coordination modes highlights its importance in elucidating the mechanistic details of photoinduced haptotropic shift reactions. Other compounds containing  $\pi$ -coordinated pyrrolyl ligands are currently under investigation.

### Experimental Section

**Materials.** All operations were performed under inert gas atmospheres, and purity of all isolated products was verified by microanalysis. Spectroscopic grade cyclohexane and toluene were used as obtained (Aldrich spectroscopic grade). Gases used for the matrix experiments and for the flash photolysis experiments (Ar, N<sub>2</sub>, and CO) were BOC research grade (99.999% purity).  $(\eta^5\text{-C}_5\text{H}_5)\text{Fe}(\text{CO})_2\text{I}$  was supplied by Aldrich

and used without further purification. The parent species,  $(\eta^5\text{-C}_5\text{H}_5)(\eta^5\text{-C}_4\text{H}_4\text{N})\text{Fe}$ , was synthesized by the method reported by Pauson,<sup>23</sup> and  $(\eta^5\text{-C}_5\text{H}_5)\text{Fe}(\text{CO})_2(\eta^1\text{-N-C}_4\text{H}_4\text{N})$  was synthesized according to the method of Zakrzewski.<sup>24</sup>

**Apparatus.** Spectra were recorded on the following instruments: IR, Perkin-Elmer 2000 FT-IR (2 cm<sup>-1</sup> resolution), UV/vis Hewlett-Packard 8452A; NMR, Bruker AC 400. The laser flash photolysis apparatus has been described previously.<sup>5</sup> For this work, both the 355 and the 532 nm lines of a pulsed Nd:YAG laser were used (energy approximately 35 and 80 mJ per pulse respectively; system response 20 ns). Solutions for analysis were placed in a fluorescence cuvette ( $d = 1 \text{ cm}$ ) attached to a degassing bulb and were degassed by three cycles of freeze–pump–thaw to  $10^{-2}$  Torr, followed by liquid pumping to remove traces of water and carbon dioxide (this typically removed half the original volume of solvent). The absorbance of the solution at the excitation wavelength was adjusted to lie in the range 0.5–1.0. The UV/vis spectrum of the sample solution was monitored throughout the experiments to monitor changes in absorbance. The concentration of CO was determined by the pressure of CO admitted to the cell. The solubilities of CO in cyclohexane and toluene are  $9.0 \times 10^{-3}$  and  $7.5 \times 10^{-3} \text{ M}$ , respectively, under 1 atm of CO at 298 K.<sup>25,26</sup>

The matrix isolation apparatus has been described in detail elsewhere.<sup>27</sup> Samples for infrared spectroscopy or for UV/vis spectra were deposited onto a CsI or BaF<sub>2</sub> window cooled by an Air Products CS202 closed-cycle refrigerator to 12–20 K. The outer windows of the vacuum shroud were chosen to match. Both  $(\eta^5\text{-C}_5\text{H}_5)(\eta^5\text{-C}_4\text{H}_4\text{N})\text{Fe}$  and  $(\eta^5\text{-C}_5\text{H}_5)(\eta^1\text{-N-C}_4\text{H}_4\text{N})\text{Fe}(\text{CO})_2$  were sublimed from right-angled tubes at 289–294 and 313–316 K, respectively, as the gas stream entered the vacuum shroud. The samples were deposited onto the windows at 20 K, which were then cooled to 12 K before recording the IR spectra on a Mattson Unicam Research Series FTIR spectrophotometer fitted with a TGS detector and a CsI beam splitter, which was constantly purged with dry CO<sub>2</sub>-free air. Spectra were recorded at 1 cm<sup>-1</sup> resolution with 128 scans. UV/vis spectra were recorded on a Perkin-Elmer Lambda 7G spectrophotometer. Matrixes were photolyzed through a quartz window with a 300 W Xe arc lamp and a water filter. Photolysis wavelengths were selected with cutoff or interference filters.

**Acknowledgment.** The authors gratefully acknowledge the support of Enterprise Ireland (D.P.H.) and CONACYT (Mexico) (V.M.P.). We also appreciate the help of Mr. V. Lafond with matrix experiments.

**Supporting Information Available:** A listing of the final refined geometric parameters and the results of a frequency calculation for the 14-electron  $(\eta^5\text{-C}_5\text{H}_5)(\eta^1\text{-N-C}_4\text{H}_4\text{N})\text{Fe}$  species. This information is available free of charge via the Internet at <http://pubs.acs.org>.

OM0002632

(23) Pauson, P. L.; Qazi, A. R.; Rockett, B. *J. Organomet. Chem.* **1967**, 7, 325.

(24) Zakrzewski, J. *J. Organomet. Chem.* **1987**, 327, C41–C42.

(25) Boese, W. T.; Ford, P. C. *Organometallics* **1994**, 13, 3525.

(26) Makrancy, J.; Megyery-Balog, K.; Rosz, L.; Rosz, L.; Patyt, D. *Hung. J. Ind. Chem.* **1976**, 4, 269.

(27) Haddleton, D. M.; McCamley, A.; Perutz, R. N. *J. Am. Chem. Soc.* **1988**, 110, 1810.

(21) Farrell, G. Ph.D. Thesis, Dublin City University, 1992.

(22) Breheny, C. J.; Kelly, J. M.; Long, C.; O'Keeffe, S.; Pryce, M. T.; Russell, G.; Walsh, M. M. *Organometallics* **1998**, 17, 3690.